Structures 37 (2022) 267–283

Contents lists available at ScienceDirect

Structures

journal homepage: www.elsevier.com/locate/structures

Seismic behavior of LRB and FPS type isolators considering torsional effects

Esra Ozer [a,*], Mehmet Inel [a], Bayram Tanik Cayci [a]

[a] Department of Civil Engineering, Pamukkale University, 20070 Denizli, Turkey

ARTICLE INFO

Keywords:
Base isolation
Torsion behavior
Lead rubber isolator
Friction pendulum isolator
Time history analysis

ABSTRACT

This study aims to investigate seismic behavior of lead-core rubber elastomeric bearing (LRB) and curved surface friction pendulum slider (FPS) base isolated models considering torsional irregularity for typical reinforced concrete buildings. Nonlinear behavior of structural members was considered in analysis models. Total of 1408 different nonlinear time history analyses of 3-dimensional 3, 5, 7 and 9-story models were performed considering 11 spectrum compatible ground motion record pairs. The results indicate that when the rigidity center of base isolator system is not coincided with mass center of superstructure, highest torsional irregularity coefficients were calculated. Lead-core rubber elastomeric bearing type isolators are more sensitive to torsional effects compared to curved surface friction pendulum slider type isolators. Torsional irregularity coefficient values of lead-core rubber elastomeric bearing models with 20% eccentricity are 47% higher than models without eccentricity in terms of averages. The obtained results indicate that significant scatter exists in displacement values of individual ground motion records for all models. Using limited number of ground motion records may lead to inaccurate predictions of seismic demands.

1. Introduction

The loss of life and property caused by many large-scale past earthquakes has increased the importance of improving the seismic performance of facilities that contain valuable equipment and must continue to be used immediately after the earthquake such as hospitals, police and radio stations and telecommunication centers, etc. Base isolation technology is nowadays used as an option in seismic zones to improve seismic performance of structures subjected to earthquakes. The control of structural movements for such buildings is carried out with a specially designed interface at the level of isolators.

The main function of seismic isolators is to reduce the transmission of shear forces to the superstructure by extending the vibration period of the whole system, while providing enough rigidity at service load levels for wind and small earthquakes [1,2]. Large displacement problems of isolation system can be eliminated by applying significant damping [3]. The desirable features of isolators are their low lateral stiffness with good energy dissipation and re-centering capability and vertical stability under the building weight and large displacements. The force–displacement behavior of typical isolator is nonlinear, hysteretic and can be idealized by either a rigid-linear, bilinear or tri-linear model [4–6]. The most common seismic isolator types in practice are high damping natural rubber bearings (HDRB), lead-core rubber elastomeric bearing (LRB) and curved surface friction pendulum slider isolators (FPS) [7,8]. LRB, FPS and HDRB type isolators are widely used in practice for building structures. Since LRB and HDRB type isolators have similar behavior, only LRB and FPS type isolators were considered in the scope of this study.

LRB type isolators consist of steel plates between multiple rubber layers and contains one or more lead cores in its center [9]. The amount of damped seismic energy increases via lead core at LRB type isolators. Curved surface friction pendulum slider type isolators (FPS) perform the pendulum-like motion of an articulated slider on a concave friction surface. These isolators become active when the earthquake demands exceed the friction force on the isolator surface. With the movement of such isolators, a lateral force occurs in the system with friction and with the rise of the superstructure on the spherical surface. While this force is directly proportional to the weight carried by the isolator, it is inversely proportional to the radius of the concave surface for the elastic component of the total force developed at the FPS which is the sum of elastic and friction components. In the inelastic FPS isolator behavior, the behavior varies depending on friction and speed [10]. Since it is not possible to define a true hysteretic loop in the modeling, various assumptions are made in the modelling of FPS type base isolators. The coefficient of friction is assumed as constant and stick–slip behavior is neglected when the direction of motion changed [11–15]. Hysteretic

* Corresponding author.
E-mail addresses: esrao@pau.edu.tr (E. Ozer), minel@pau.edu.tr (M. Inel), bcayci@pau.edu.tr (B.T. Cayci).

https://doi.org/10.1016/j.istruc.2022.01.011
Received 2 September 2021; Received in revised form 26 December 2021; Accepted 4 January 2022
Available online 11 January 2022

loop, maximum geometric displacement and extra-stroke displacement capacity are deviated from real behavior because of the assumptions made in design stage [16,17].

Conventional FPS is essentially rigid under pressure and has no tensile load capacity while LRB has relatively less compressive stiffness and can withstand a limited amount of tensile load [18]. The huge disadvantage of the LRB type isolator is that the damage to the central lead core cannot be determined after a strong ground motion. Moreover, there is no self-re-centering feature as in the FPS type isolator. The similar behavior would be expected for the base isolated models with same isolation period and damping ratio. However, seismic response of superstructure is also affected by the general characteristics of isolation model and the differences can be observed in certain cases [19–22]. FPS type isolators are more stable against unwanted differences in the and dynamic amplification effects of ground motions. The lateral force generated by FPS type isolators which is proportional to the weight of the structure provides to coincide the mass center of the building with the rigidity center of the isolator system. This feature, proved in shake table tests by Zayas et al., eliminates the torsional effects that may occur [23,24].

The most important advantage of the LRB type isolator over the FPS type isolator is that it is a well tried and tested device since their prototype and production tests can be carried out in a limited number of centers around the world compatible with certain standards. Another important advantage of the LRB type isolator is that it does not have high initial friction that causes high accelerations in the system and a variable friction coefficient at high speed that causes the accepted hysteretic behavior to be far from the real behavior [10]. In addition, the lead core provides elastic rigidity to the system at small amplitude earthquakes or winds.

Previous research has generally focused on investigating a single type of base isolation system [25–27] instead of comparing different isolator systems in the same study (such as Hoseini Vaez et al. 2012 [22]). Apart from these, many previous studies have used models with different eccentricities derived from one benchmark three-dimensional (3D) model. In addition, many superstructure models used to examine dynamic behavior are generally elastically designed. The studies used either few (3 records) records or considerable number of records for a specific region or specific earthquake [28–30]. For example, Becker et.al [31] studied only one type of eccentricity of the superstructure considering 3 different eccentricity ratios (0%, 17% and 25%) for only one of type isolator (Triple Pendulum System (TPS) which is an effective isolator against torsion). One-directional seven earthquake record were selected and used for time history analysis. Only the isolator displacement was examined. No correlation was observed between the increase in eccentricity and the increase in displacement in both analytical and experimental models. Besides nonlinear behavior of superstructure members was ignored. Torsional amplifications for models without eccentricity were investigated by Almazan et.al [32]. Even though the building is symmetrical, the rate of torsional magnification was determined by stating that accidental eccentricity may occur at the interface of the FPS type isolators due to the overturning effect in the event of bi-directional earthquake. A single three-dimensional superstructure model was used, and nonlinear behavior of superstructure members was ignored. In the study by Jangid and Kelly, uneven stiffness distribution of isolators was compared for 5% eccentricity ratio in terms of complete quadratic combination (CQC) and the square root of the sum of squares (SRSS) methods [33]. The two degree of freedom system (2DOF) model were used. An evaluation independent of isolator type had been made and nonlinear behavior of structural members was ignored. When mentioned studies are examined, torsional amplifications are evaluated by using a single type of isolator for a single eccentric case (for example, only superstructure mass center (CM) welded or only superstructure rigidity center (CR) welded) and for limited number of ground motion records.

Although there are many previous studies on the development and use of isolator systems, limited number of them focused on torsional irregularity effects [34]. When column layout is not symmetrical in plan or stiffness characteristics of base isolators varies, torsional effects in the structure inevitably occur under seismic loads. While some previous studies indicate that torsional effects have significant role on building response [35,36] other studies have concluded that these effects are negligible [34,37–40].

Torsional irregularity in base isolated systems may occur in new or existing buildings due to many different reasons (architectural requirements, changing purpose of use etc.). It has great importance to determine which ratio of torsional irregularity can be allowed in design stage. Since the significant part of seismic demands are eliminated by isolator system the torsional effects due to mass and rigidity center location of superstructure are expected to be limited in the base isolated systems. However, if the isolator rigidity center and superstructure mass center are not coincided, torsional effects are more critical on seismic response. In the studies, the safe distance between these centers and the effects on seismic response of base-isolated systems are still discussing.

Inherently, the mass centers and rigidity centers are well adjusted in design stage accordance with seismic code provisions and possible effects of torsional behavior are considered. But mass center of superstructure can be deviated in certain conditions like changing in the use of purpose. In this case, unexpected additional forces may be experienced in the system due to accidental torsion. Also, the plan geometry may not allow the coincidence of isolator rigidity center and superstructure mass center for existing buildings.

This study aims to evaluate the seismic behavior of LRB and FPS type base isolated models considering torsional irregularity for typical RC buildings. The possible torsional effects on superstructure due to irregular superstructure and irregular isolator placement are investigated. Torsional irregularity coefficient is used to determine the most critical case. Although building system with base isolators generally remains in elastic limits, nonlinear behavior of structural members was also considered in order to observe probable yielding of structural members in superstructure due to the torsional irregularity.

Dynamic analyses were performed by using 11 different bi-directional ground motion pairs applied at two horizontal directions, simultaneously to achieve a detailed investigation on the dynamic response of LRB and FPS base isolator systems with torsional irregularity.

2. Modelling

2.1. Reference building models

In the scope of the study, four different 3-dimensional (3D) Reinforced Concrete (RC) frame building models, were designed in accordance with the 2018 Turkish Building Earthquake Code (TBEC-2018) [41] without any structural irregularities as 3, 5, 7 and 9-story. In building design, elastic design spectrum with a return period of 475 years defined as DD-2 level earthquake in TBEC-2018 is used. These models are fully symmetrical for both orthogonal axes. Plan views of 3, 5, 7 and 9-story building models are given in Fig. 1. Typical story heights are 3.2 m and the same for all stories. Compressive strength of concrete and yield strength of steel values are assumed to be 30 and 420 MPa, respectively. The buildings used in the study were assumed to be located near Pamukkale University in Denizli, Turkey on soil type ZC that is similar to soil type C of FEMA-450[42]. The structural models are typical beam-column RC frame buildings with no shear walls. The column and beam dimensions are provided in Table 1.

SAP2000 program [43] was used for the modelling and analysis of buildings. SAP2000 has a tool to apply base isolator devices at the bottom of structure. Type of base isolator and initial parameters can be correctly defined in numerical models as used by many research studies [25,44,45]. Beam and column elements are modeled as nonlinear frame elements with lumped plasticity by defining plastic hinges at both ends

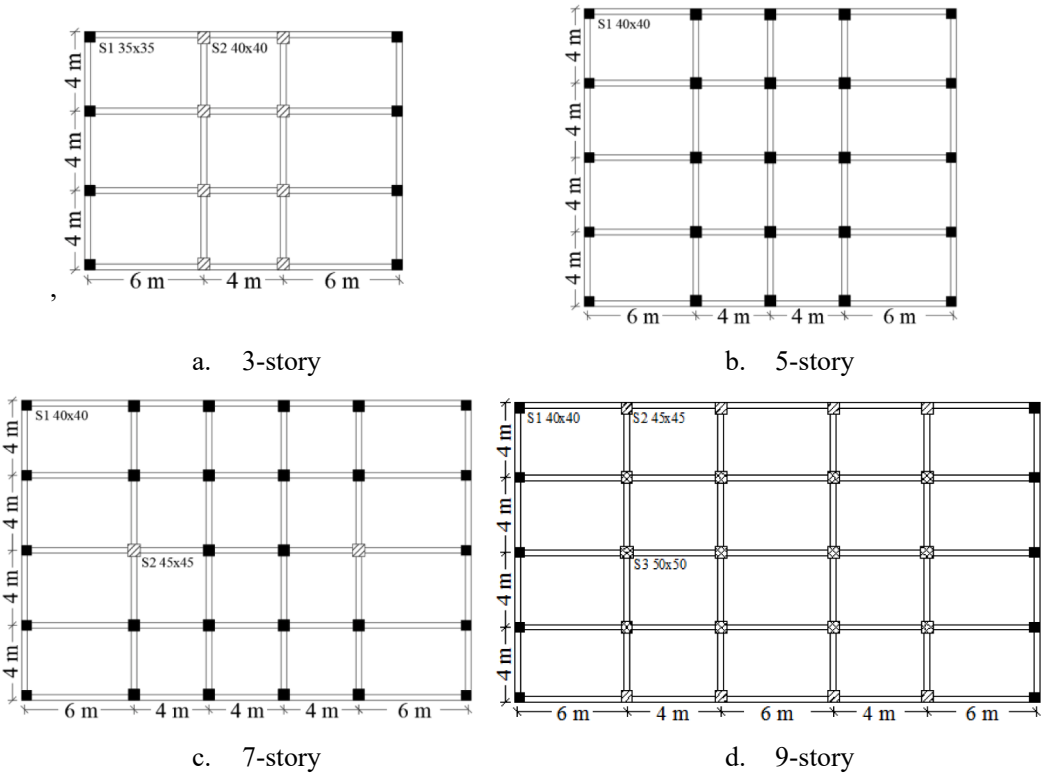

Fig. 1. Plan view of the considered buildings.

Table 1
The dimensions of the carrier system element.

Model	3-Story	5-Story	7-Story	9-Story
Beam Elements (mm × mm)	300 × 500	300 × 500	300 × 500	300 × 500
Column Elements (mm × mm)	350 × 350	400 × 400	400 × 400	400 × 400
	400 × 400		450 × 450	450 × 450
				500 × 500

of beams and columns. SAP2000 provides both the use of default hinge and user-defined hinge property options [43]. The user-defined hinge properties are used in this study [46]. In the critical sections of the beams and column members, moment–curvature analyzes were performed by considering the dimensions, longitudinal and transverse reinforcement contents and axial load levels using SEMAp program [47]. Rotation values required for the nonlinear analyses were defined in the SAP2000 program used in the modeling and analysis stages [43]. Plastic hinges at column members were applied considering M2-M3 interaction since time history analyses performed as bi-directional. The effective section stiffness of column and beam members were defined 0.70EI and 0.35EI as defined in TBEC-2018 [41] respectively. The capacity curves of the considered fixed-base models are given in Fig. 2.

2.2. Isolator models

LRB and FPS type base isolator systems were considered in the scope of this study. The base isolated models were created by placing the isolators on the base level of the conventional 3, 5, 7 and 9-story buildings. Models with isolators are diversified with only LRB and only FPS models. An isolator is placed under each column.

In the iterative design process, four main points were taken into account. First, the period of base isolated models should be at least 3 times longer than that of the fixed-base model. Secondly, the obtained maximum lateral displacement values of each analysis case should be lower than the determined D_{max} value. Thirdly, lowest possible damping rate in the range of 15–30% should be considered and finally, the determined D_{max} value should be higher than minimum allowable displacement value defined in TBEC-2018 [41].

The desired damping amount is achieved more easily with the lead core placed at the center of the rubber type isolators (LRB) [9]. Typical view of LRB type base isolator model is shown in Fig. 3a. The hysteretic behavior of the LRB isolator can be idealized as bi-linear, shown in Fig. 3b. The parameters on the figure are characteristic strength (F_Q), initial (elastic) rigidity (k_1), secondary (inelastic) rigidity (k_2), effective stiffness (k_e) corresponding to the horizontal force (F) and isolator displacement (D), effective yield strength (F_y), and effective yield displacement (D_y). The design of LRB type isolators is summarized in the design flowchart given in Fig. 4. According to design chart, the maximum axial load on the columns is determined by static analysis of the fixed-supported structure under vertical loads. The effective cross-sectional area A_0 of the bearing based on the allowable axial stress under the vertical load case of dead load plus live load (P_{DL+LL}) was computed. The effective cross-sectional area A_1 of the bearing from the shear strain due to the vertical load P_{DL+LL} was determined. The target design period T_D for the isolated structure and maximum allowable displacement values restricted by field conditions D_{max} of the bearing were selected.

The effective horizontal stiffness K_{eff} and maximum horizontal (design) displacement D of the bearing were determined by using the code formulas or static/dynamic analysis. The effective damping ratio ξ_{eff} for the bearing was selected compatible with D_{max} and T_D. The material properties, including Young's modulus E, shear modulus G and design shear strain γ_{max} from the manufacturer's test report were selected. The total height of rubber layers, t_r, corresponding to the

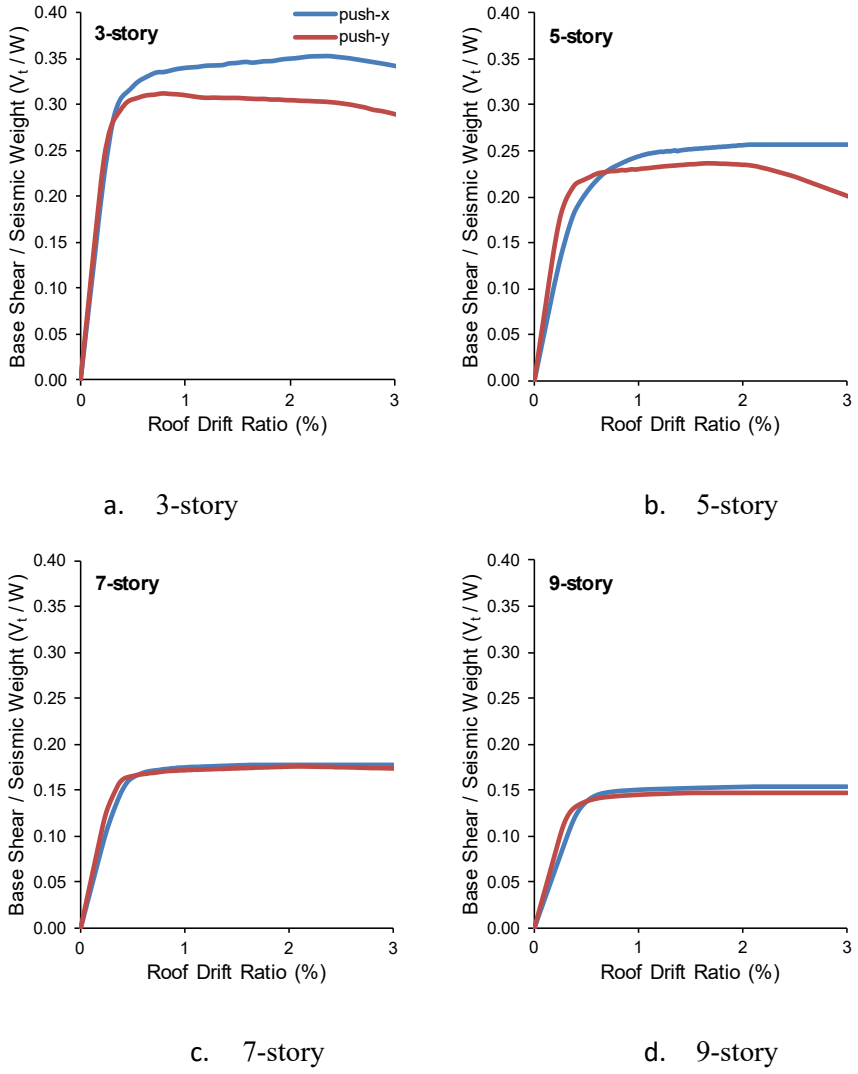

Fig. 2. Capacity curves of fixed-base models.

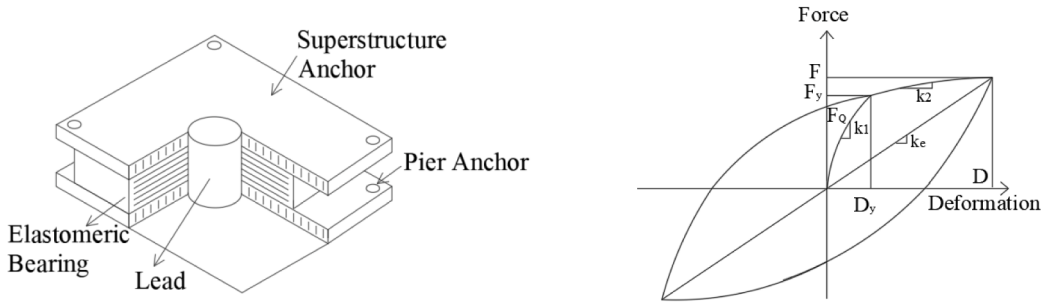

a. Laminated rubber bearing with lead core

b. Idealized bilinear force-displacement relation of lead rubber isolator

Fig. 3. Lead core laminated rubber bearing parts and its hysteresis model [41].

design displacement D and design shear strain γ_{max} was calculated. Then, the effective cross-sectional area A_2 as the reduced area A_{re} according to code formulas was computed. The design cross-sectional area A of the bearing is taken as the maximum among the three values computed: A_0, A_1 and A_2.

The thickness of individual rubber layer, t, from the shape factor S and dimensions of the rubber layer was determined. Steel plate thickness, t_s was calculated by means of the previously defined parameters

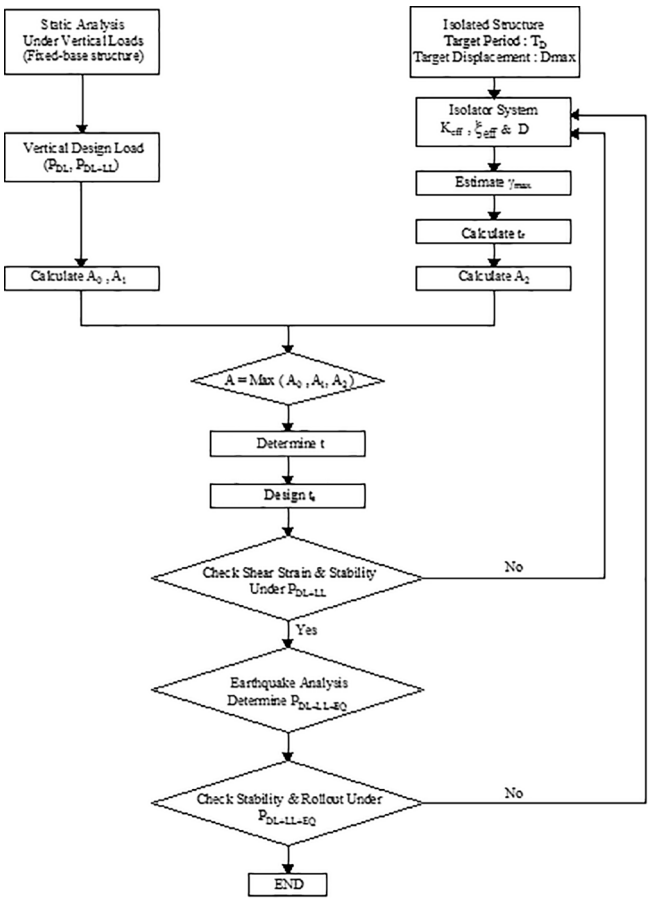

Fig. 4. Design flowchart for LRB type isolators.

and code formulas. Shear strain condition for the normal load case should be satisfied. Shear strain and stability conditions were checked through code formulas. If the dimensions determined for the bearing cannot satisfy the shear strain and stability requirements or D_{max} is exceeded for any earthquake condition, design steps were repeated for an improved design.

Fig. 5 shows the FPS isolator and its hysteretic behavior. Unlike the hysteretic behavior of the LRB isolator, the parameters that make up the curve, F_Q and F_y are the same values and are equal to the product of the effective friction coefficient (μ) and the vertical force (P) acting on the isolation unit. Besides, the values of k_2 and k_e depend on the effective radius of curvature (R) of the curved frictional isolation unit sliding surfaces. The design of FPS type isolators is summarized in the design flowchart given in Fig. 6. For FPS models, the target design period T_D for the isolated structure and maximum allowable displacement values

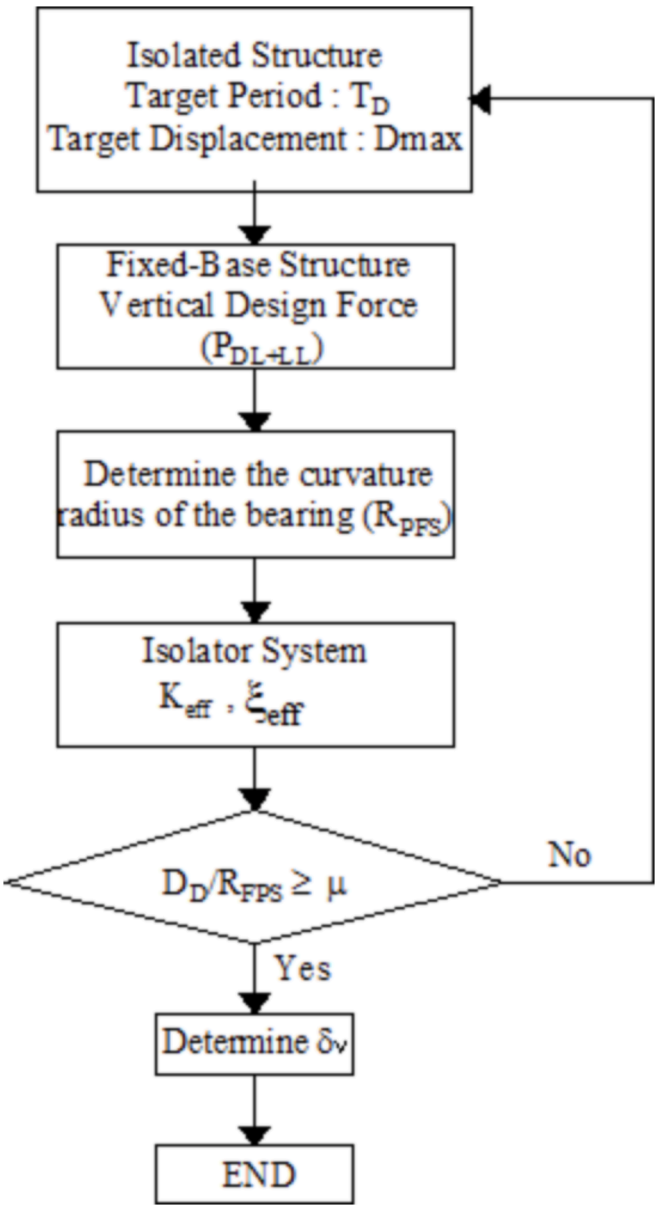

Fig. 6. Design flowchart for FPS type isolators.

restricted by field conditions D_{max} of the bearing were selected. In design of the frictional pendulum bearing, one key concern is to make the natural period T_D long enough, such that the forces transmitted from the ground to the superstructure can be greatly reduced. For this reason, T_D

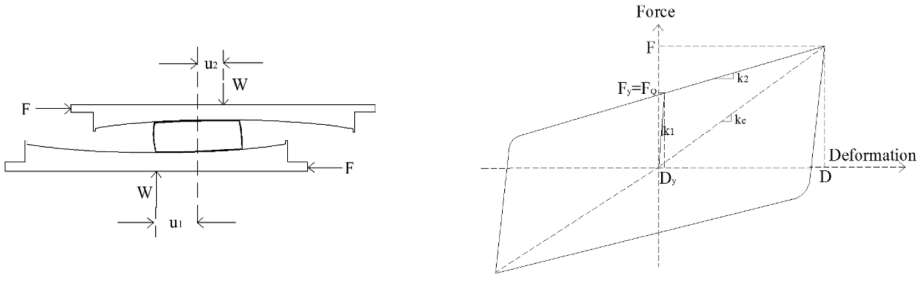

a. Friction pendulum system

b. Idealized rigid-linear force-displacement behavior of FPS isolator

Fig. 5. Curved surface friction pendulum isolator parts and its hysteresis model [41].

has been chosen at least 3 times larger than the period value of the fixed-base model. The maximum axial load on the columns is determined by static analysis of the fixed-base structure under vertical loads. In addition, the period T_D of the friction pendulum system (FPS) isolated structure can be designed through a proper choice of the radius of curvature, R_{FPS}, for the spherical sliding surface. The effective stiffness of the isolator (K_{eff}) is calculated in accordance with the code formulas by using the maximum axial loads on each column, the R_{FPS} of the curved surface friction isolator and the friction coefficient (μ) and maximum horizontal (design) displacement D_D of the bearing. The effective damping ratio ξ_{eff} provided by the isolation system is also a function of the design displacement (D_D), R_{FPS} and μ. The vertical displacement δ_v of the structure caused by the curved surface of the isolator was estimated by code formulas. To ensure that the isolated structure will return to its original position, the horizontal displacement D_D of the structure under the earthquake load should meet the requirement that the restoring force is not less than the friction force. Finally, when it was determined that the design displacement (D_D) did not exceed D_{max} in all earthquake situations, the iterative design process was terminated.

The design parameters of the isolator used in this study for the SAP2000 program [43] are summarized in Table 2. These parameters were determined according to maximum lateral design displacement value (D_{max}) given in Table 2. The total stiffness capacity of isolator systems with eccentricity was taken same as models without eccentricity to better observe the torsional effects. In Table 2, the parameters are as follows: P_{DL+LL}; the maximum axial load to be carried by the isolator due to dead and live loads, d_p; the lead core diameter, d; rubber diameter, t_r; the total rubber height, K_v, K_e, K_1 and K_2 the vertical, effective, initial and secondary stiffness of the isolator, F_y; yield strength, ξ_{eff}; effective damping, μ; coefficient of friction, R; effective radius of the curved frictional isolation, D_{max} represents maximum lateral design displacement value (it is also defined as "D" by other seismic codes) of isolators. Maximum lateral displacement value is affected by various parameters such as area restrictions, design code regulations and characteristics of superstructure. In the scope of this study D_{max} value is assumed equal to minimum allowable displacement value defined in TBEC-2018 [41].

2.3. Torsional irregularity

The structure in the base isolation system is idealized as a rigid platform with masses lumped in corresponding column positions as shown in Fig. 7a. The base deck, which is considered to have a rigid diaphragm behavior, is supported by massless isolators. The center of rigidity (CR) of base isolation system may not coincide with center of mass (CM) of the superstructure in certain cases such as accidental torsion and design restrictions [33]. In this case, additional torsional moments can occur due to the earthquake force, with the force arm equal to the distance between CR and CM. As a result, the lateral movement of the system is combined with the torsional motion that can be occurred in both transverse directions. Torsional irregularity in building models were created by changing the eccentricity between mass centers and rigidity centers of system at X direction since building models have lower stiffness at that direction.

TBEC-2018 [41] and all other similar seismic codes [48,49] state that torsional irregularity in the plan should be avoided in base isolated buildings. Because it can lead negative impact on the seismic behavior of the building. The definition of torsional behavior in TBEC-2018 is illustrated in Fig. 7b. According to TBEC-2018 [41], if the torsional irregularity coefficients (η_{bi}) given in Eq.1 is greater than 1.2, torsional irregularity exists in the structure. $\Delta_{i,max}$ and $\Delta_{i,min}$ are the maximum and minimum relative story displacements at the story level i. The average relative story displacement ($(\Delta_i)_{average}$) is calculated as given in Eq. (2). Although there are constraints on torsional irregularity for superstructures in TBEC-2018 [41], no restriction exists in the design of base-isolated systems.

$$\eta_{bi} = \frac{(\Delta_i)_{max}}{(\Delta_i)_{average}} > 1.2 \tag{1}$$

$$(\Delta_i)_{average} = \frac{(\Delta_i)_{max} - (\Delta_i)_{min}}{2} \tag{2}$$

Table 2
Design parameters of the used isolators.

Parameters	Unit	3-Story LRB	5-Story LRB	7-Story LRB	9-Story LRB
P_{DL+LL}	kN	320	682	870	1327
d_p	mm	43	67	70	71
d	m	0.40	0.55	0.60	0.70
t_r	m	0.65	0.65	0.75	1.00
K_v	kN/m	98,399	186,035	192,520	440,057
K_e	kN/m	143	305	294	252
K_2	kN/m	98	209	202	173
F_y	kN	14.7	31.3	34.2	39.7
K_2/K_1	–	0.69	0.54	0.5	0.46
ξ_{eff}	–	0.15	0.20	0.22	0.25
D_{max}	m	0.35	0.40	0.40	0.45
Parameters	Unit	3-Story FPS	5-Story FPS	7-Story FPS	9-Story FPS
P_{DL+LL}	kN	320	682	870	1327
K_e	kN/m	99	445	622	676
K_2	kN/m	76	99	85	124
μ	–	0.03	0.03	0.03	0.03
R	m	2.24	2.24	3.05	4.24
ξ_{eff}	–	0.20	0.24	0.27	0.29
D_{max}	m	0.35	0.40	0.40	0.45

3. Ground motion records

Within the scope of the study, a total of 11 ground motion record pairs were selected from the PEER Ground Motion Database of the Pacific Earthquake Engineering Research Center [50]. Both components of these records (H_1 and H_2) were scaled according to the elastic acceleration spectrum for 5% elastic damping ratio defined in TBEC-2018 [41]. Scaling process was conducted using spectral matching, which is the most recommended earthquake record selection method for seismic codes [51].

The advantage of using spectrum matching is that the dispersion among analyzes is reduced and it enables a realistic estimation of the average response using less ground motion records [52,53]. The design parameters were determined according to the location of the building as defined in TBEC 2018 [41]. The spectral parameters used for this location are given in Table 3 for the design earthquake with 10% probability of exceedance in 50 years. In the table, the short-period design spectral acceleration coefficient and the design spectral acceleration coefficient for the 1.0 s period are expressed as S_{DS} and S_{D1}, respectively. The short-period map spectral acceleration coefficient and the map spectral acceleration coefficient for the 1.0 s period are expressed as S_S and S_1, respectively. The equivalents of the soil parameters S_{DS}, S_{D1}, S_S and S_1 in the TBEC-2018 are stated that S_{MS}, S_{M1}, S_S and S_1 in the FEMA-P-1051 [5], respectively.

The rules for the selection and scaling of ground motion records considering TBEC-2018 [41] criteria's are given below:

- Magnitude: $6.0 \leq Mw \leq 7.5$
- Closest distance to the rupture surface: $10 \leq R_{rup} \leq 30$
- Vs30: $360 \leq V_s30 \leq 760$ for the selected site soil type
- Fault mechanism (strike slip, normal, reverse)
- No pulse-like records
- 3D time history analysis requires at least 11 pairs of ground motion records, not exceeding three record pairs from the same earthquake event.
- The same scale factor is applied in both horizontal components of the records.

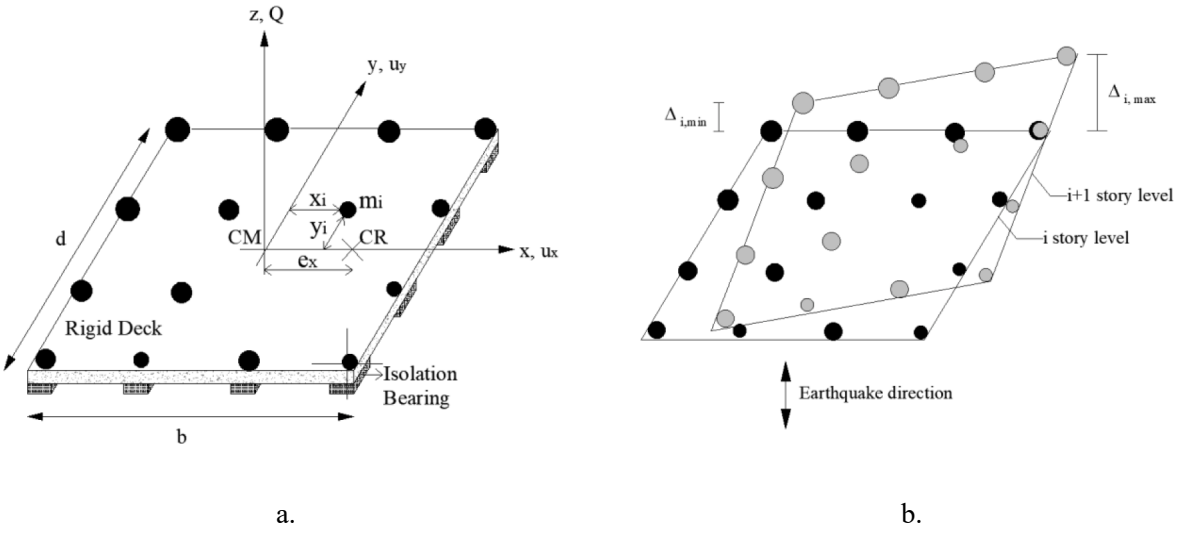

Fig. 7. Torsional irregularity case [41].

Table 3
Ground parameters of design earthquake level (DD-2) for building location [41].

Parameters	Value
S_1	0.261
S_S	1.135
S_{D1}	0.658
S_{DS}	1.135

- The mean spectrum obtained as square root of sum of squares for the scaled ground motion records shall not be less than 1.3 times the target design spectrum between $0.5T_M$ and $1.25T_M$ periods for the base isolated buildings, where T_M refers to the effective vibration period of building with seismic isolator subjected to the highest possible displacement.
- The ordinates of the site-specific earthquake ground motion spectra are never smaller than 90% of the design spectrum (horizontal elastic spectrum) ordinates.
- The nonlinear analyses in the scope of this study should be performed as bi-directional.

The obtained elastic acceleration spectrums are illustrated in Fig. 8 for the 5% damping ratio for the selected records. In addition, the spectrum of TBEC-2018 on the ZC soil type with a probability of exceeding 10% in 50 years and the average of the ground motion records were plotted on the same figure. Although the scatter of the selected records is high, the average values are very close to the TBEC-2018 spectrum requirement (1.3 times design spectrum). It should be noted that TBEC-2018 does not contain any conditions restricting the standard deviation from the mean elastic spectrum. The properties of the ground motion records used are given in Table 4.

4. Results and discussion

4.1. Modelling effect on torsional irregularity

In order to determine the most critical torsional irregularity condition, four different cases were created by changing the positions of the

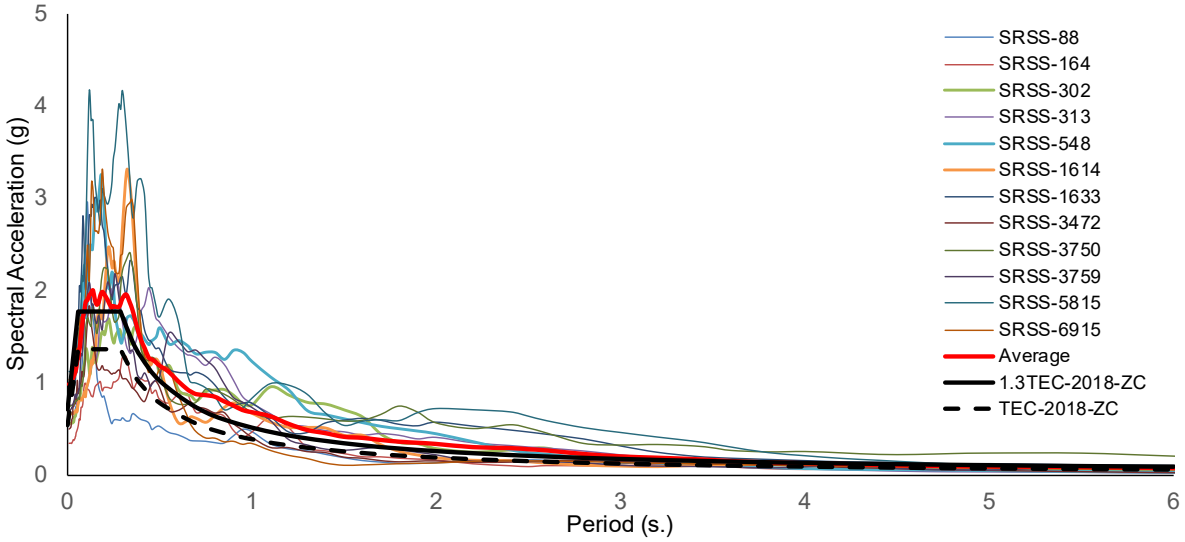

Fig. 8. Elastic acceleration spectrum for 5% damping of ground motion records used in the study.

Table 4
Ground motion record properties used in the study [50].

No	RSN	Earthquake	Year	Location	Mw	Componenet H_1-H_2	PGA (g)	Vs30 (m/s)	Scale Factor
1	88	San Fernando	1971	Santa Felita Dam	6.6	000–090	0.387	389.0	2.5
2	164	Imperial Valley-06	1979	Cerro Prieto	6.5	000–090	0.252	471.5	1.5
3	302	Irpinia_ Italy-02	1980	Rionero In Vulture	6.2	000–270	0.399	574.9	4.0
4	313	Corinth_ Greece	1981	Corinth	6.6	000–090	0.592	361.4	2.0
5	548	Chalfant Valley-02	1986	Benton	6.2	270–360	0.733	370.9	3.5
6	1614	Duzce_ Turkey	1999	Lamont 1061	7.1	E-N	0.525	481.0	4.0
7	1633	Manjil_ Iran	1990	Abbar	7.4	000–090	0.617	724.0	1.2
8	3750	Cape Mendocino	1992	Loleta Fire Station	7.0	270–360	0.531	515.7	2.0
9	3759	Landers	1992	Whitewater T.Farm	7.3	180–270	0.494	425.0	4.0
10	5815	Iwate_ Japan	2008	Yuzawa	6.9	EW-NS	0.791	655.5	4.0
11	6915	Darfield_ N.Zealand	2010	Heathcote V. PS	7.0	000–090	0.930	422.0	1.2

mass and rigidity centers of the isolator and the building for 3-,5-,7- and 9-story models (Fig. 9). Models with isolators are diversified with only LRB and only FPS models. 704 different nonlinear time history analyses of 32 different models were performed considering 11 pairs of spectrum compatible record set. In Fig. 9, E_q, e_{bx} and M represents seismic force, static eccentricity and moment, respectively.

The rigidity center (CR_i) and mass center (CM_i) of the isolators coincide with the superstructure rigidity center (CR_b) and mass center (CM_b) without any torsional irregularity for Case 1 and named as zero eccentricity (e0) models. In general, seismic codes, provisions and many other authors (except Kilar and Koren 2009 [29]) recommend that Case 1 should be provided as much as possible in the design of isolated buildings in order to avoid possible torsional behavior [35,36,41,54,55].

The second case (Case 2) represents the irregular stiffness distribution in the superstructure with 20% eccentricity ($e_{bx}/L = 0.2$) named as e20. The eccentricity of the superstructure rigidity center was obtained by increasing the dimensions of the x direction columns of exterior axis. The rigidity center of isolators coincides with the superstructure mass center (CM_b) as recommended in the design phase.

The Case 3 and Case 4 are obtained from Case 1 and Case 2 by shifting the location of the superstructure mass center (CM_b) due to possible changes in the purpose of use of the existing building. Although it is not encountered during the design stage, it represents base isolated models whose purpose of use was changed later. In fact, in the design phase, the isolator rigidity center is considered as close as possible to the building mass center in order to minimize possible torsional effects in the superstructure with an irregular mass distribution.

The base isolated models were created by placing the isolators on the base level of the conventional 3, 5, 7 and 9-story building models. LRB and FPS type base isolation systems were designed with 0% and 20% of plan dimension eccentricity between mass center of superstructure and rigidity center of base isolation system. Models with torsional irregularity were designed by changing the horizontal stiffness of the isolators to obtain 20% of plan dimension of building distance between rigidity center of isolators and mass center of superstructure. The total lateral isolator stiffness was considered as constant in models with torsional irregularity as described in Fig. 10 where *ki* represents isolator stiffness.

Since the x-direction of buildings is more sensitive to torsional effects, the unidirectional eccentricity in x-direction (e_x) was created at the isolator interface. This study considers the most critical case, e_x-eccentricity of the system in the x-direction as mentioned above. The same target displacement value was used at design stage to compare the effect of torsional irregularity and base isolator types on seismic response, properly.

The building model properties are summarized in Table 5 as total seismic weight(W) and base shear force values (V_{tx} and V_{ty}). The terms of T_x, T_y and T_z correspond to the x- direction, y-direction and torsional mode period of system. The period shifting is obvious for base-isolated system compared to fixed-base models. As given in Table 5, building models with LRB and FPS type isolators have different dominant period and damping value for the same maximum design displacement value. For that reason, the obtained results are also affected by the difference in dynamic properties of LRB and FPS type isolators determined in design stage. If LRB and FPS type isolators have the same period and damping values, the difference in the obtained demands are expected to be minimum. However, from the perspective of design process, the same maximum displacement value should be considered for different type of base isolators since it is related with field conditions, superstructure properties and definitions of seismic codes rather than the base isolator type. The differences in period and damping ratio values for the same design displacement value is an indicator of response characteristics of LRB and FPS type isolators.

Nonlinear time history analyses were carried out for the four cases described above subjected to 11 ground motion pairs. The most critical case was determined based on the torsional irregularity coefficients of the superstructure calculated from the obtained results. When the coefficients shown in Fig. 11 are examined, it is obvious that the average values are below 1.2 except Case 4 (C4). However, the 1.2 value was exceeded for limited number of individual ground motion records for the first three cases. This study also illustrates that Case 2 is more critical than Case 3 for LRB type isolators contrary to the study by Tena-Colunga and Escamilla-Cruz [30]. It should be also noted that, torsional irregularity coefficients are higher for FPS type isolators compared to LRB type isolators for Case 1, 2 and 3 except 9-story Case 2 e20 model. Since the isolators are placed symmetrically for the first 3 cases, the existing irregularities are caused by the superstructures. For this reason, the fact that the torsional coefficients of the models with FPS type isolators in the first 3 cases are slightly higher than the models with LRB type isolators are related to the superstructure rather than the type of isolator. However, it should be noted that a large torsional irregularity coefficient does not always indicate critical translation values. The obtained results indicate that the acceleration values of the models with 3,5 and 7-story LRB and FPS type isolators show greater variation depending on the period value in the elastic design spectrum. However, this difference is

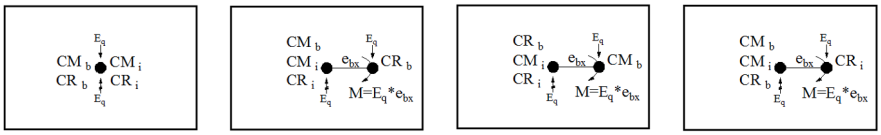

a. Case 1 (C1) b. Case 2 (C2) c. Case 3 (C3) d. Case 4 (C4)

Fig. 9. Plan view of the center of mass and center of rigidity of considered models.

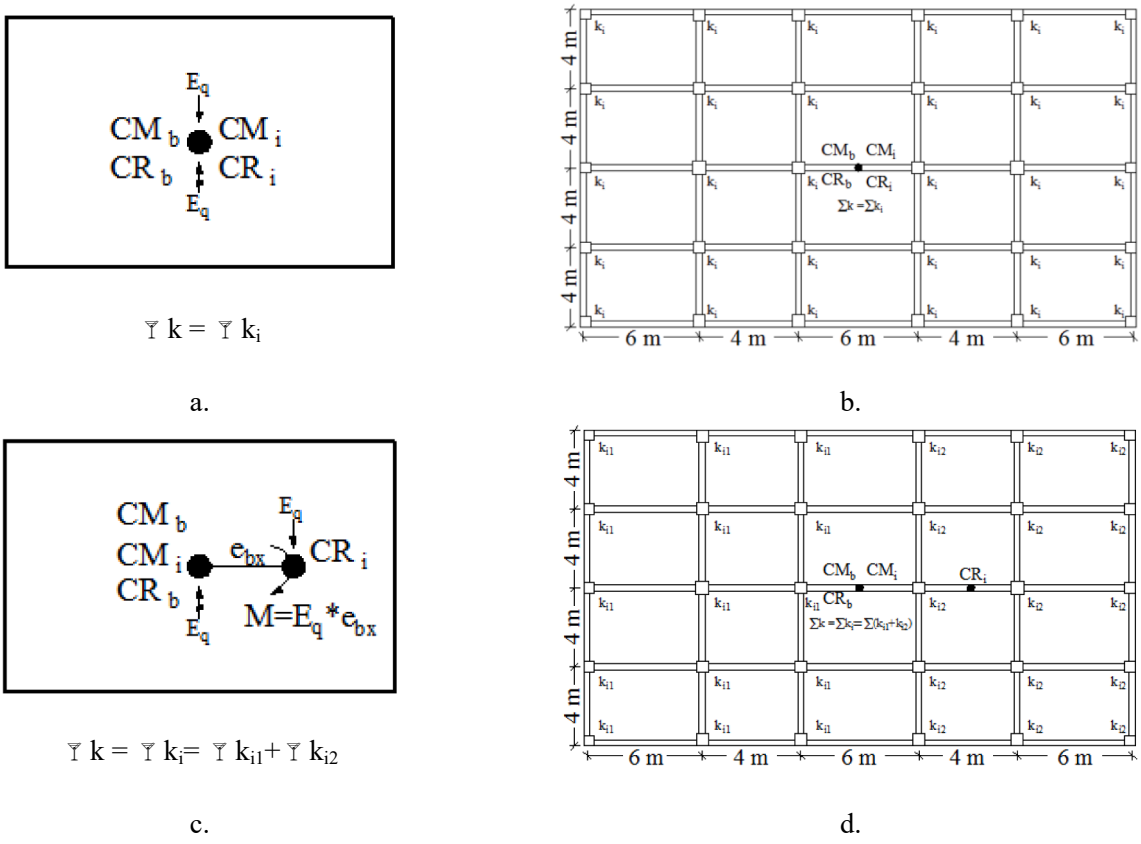

Fig. 10. Plan view of the center of mass and center of rigidity of considered models.

Table 5
Comparisons of model parameters.

Model		3-story	5-story	7-story	9-story
Fixed	Tx (s)	0.51	0.87	1.15	1.51
	Ty (s)	0.48	0.82	1.12	1.34
	Tz (s)	0.47	0.78	1.05	1.32
	W (kN)	4623.6	12753.8	19885.5	32623.2
	V_{tx} (kN)	1549.8	3200	3472.6	4836.1
	V_{ty} (kN)	1399.7	2996.7	3009.6	4565.2
e0 LRB	Tx (s)	2.98	3.34	5.01	5.51
	Ty (s)	2.36	3.32	4.84	5.18
	Tz (s)	1.95	3.15	4.24	4.87
e0 FPS	Tx (s)	2.58	3.03	4.05	4.82
	Ty (s)	2.01	2.94	3.62	4.02
	Tz (s)	1.69	2.37	2.97	3.61

almost negligible in the 9-story model. Since the displacement and period values are almost the same for 9-story LRB and FPS type isolator type models, it is thought that it can be an indicator of a comparison according to the isolator type. The difference in irregularity coefficients seems to be limited for the first three cases. However, torsional irregularity coefficients are significantly higher for Case 4 compared to the other cases. The average values are above the 1.2 limit in all models both for LRB and FPS type isolators. Besides, significantly higher scatter is apparent for each ground motion record. The outcomes underline that when mass center of building and rigidity center of isolators are not coincided, torsional behavior on superstructure seems to be inevitable. For this reason, Case 4 is considered as the most critical case in torsional irregularity. The behavioral difference of base isolated models is compared for different eccentricity values with Case 1 which is recommended by the code regulations.

4.2. Detailed analysis for the most critical case

A detailed evaluation of torsional irregularity on seismic response of models was carried out for Case 1 described by seismic code regulations and Case 4 which is obtained as the most critical case with the highest torsional irregularity coefficients in the previous section. The 10% eccentricity case ($e_{bx}/L = 0.1$) named as e10 is considered in addition to the analyses in the previous section. Thus, nonlinear time history analyses of 3, 5, 7 and 9-story buildings with LRB and FPS type base isolation systems are evaluated for Case 1 (without eccentricity, e0) and Case 4 (with 10 and 20% eccentricity: e10 and e20).

In the scope of this section, 528 nonlinear time history analyses for e0 and e20 models and 176 additional analyses for e10 models in previous section have been carried out. Seismic response of building models with seismic isolators are compared using maximum displacement and interstory displacement values. The obtained maximum displacement values are normalized by building height while the maximum interstory displacement values are normalized by story height to obtain “roof drift ratio (RDR)” and “interstory drift ratio (IDR)” values, respectively.

4.2.1. Evaluation of displacement values

The displacement values at the base isolation and roof level of the base isolated building models without eccentricity subjected to the scaled ground motion records are listed in Table 6 for LRB and FPS type isolator models. The roof displacement value ratios are also compared in Fig. 12. The figure illustrates that FPS type base isolated buildings tend to have higher roof drift values compared to the LRB type base isolated buildings. This is related to the lower period of FPS type isolators resulting in higher spectral demands.

The roof level displacement value ratios for e10 and e20 models normalized by e0 (u/u_{e0}) models are illustrated in Fig. 13. The symbol of “u” corresponds to displacement value of the e10 and e20 models, and

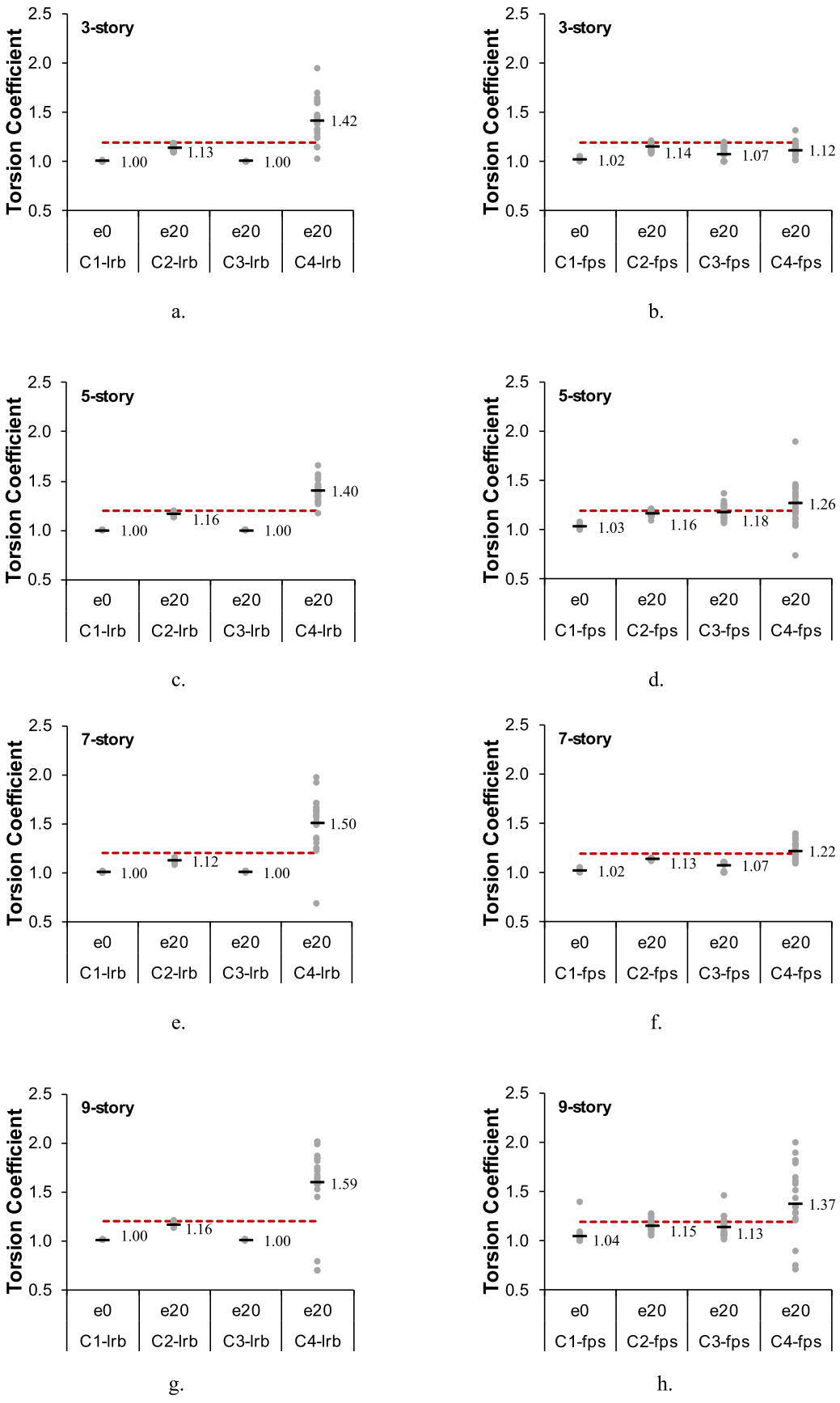

Fig. 11. Torsion coefficient (η_b) for cases.

Table 6
The displacement values at the base isolation and roof level of the base isolated buildings without eccentricity models.

RSN	Roof Displacement (mm)								Isolator Displacement (mm)							
	LRB				FPS				LRB				FPS			
	3-story	5-story	7-story	9-story	3-story	5-story	7-story	9-story	3-story	5-story	7-story	9-story	3-story	5-story	7-story	9-story
88–0	74.7	88.7	87.0	97.7	124.1	171.0	132.4	232.6	69.3	81.9	77.0	88.5	117.9	159.7	123.5	221.6
88–90	173.4	192.6	227.2	225.5	177.3	199.8	302.7	363.1	161.4	179.0	204.7	207.5	165.0	186.2	275.6	335.2
164–0	113.6	128.5	151.2	161.8	122.6	133.3	208.6	275.0	105.5	118.7	133.3	149.4	115.7	122.1	190.1	257.6
164–90	71.0	79.7	86.7	92.2	122.5	139.0	164.9	184.6	65.8	72.8	77.1	83.6	115.9	132.4	151.5	170.4
302–0	79.5	86.4	89.6	73.4	114.6	155.3	189.1	231.2	74.0	79.6	79.7	68.2	109.0	148.7	174.2	214.2
302–90	197.1	230.7	239.7	270.2	222.9	325.0	371.0	320.3	183.7	214.3	215.1	248.1	207.1	300.7	334.5	293.5
313–0	138.1	176.8	163.4	130.4	194.2	259.2	168.8	236.3	128.5	162.6	147.5	121.3	182.1	236.5	155.7	217.4
313–90	185.4	241.4	208.7	170.2	279.1	327.8	220.2	252.2	172.6	225.5	185.3	155.0	259.7	305.8	201.0	232.4
548–0	112.2	132.3	115.8	111.7	135.0	171.6	154.8	151.8	104.2	121.0	102.7	96.5	127.2	160.7	139.2	140.6
548–90	147.2	188.3	164.5	164.7	207.2	266.6	255.4	189.3	136.8	174.5	148.7	152.8	192.4	248.1	234.2	180.8
1614–0	137.5	131.8	172.0	227.9	162.5	145.2	202.9	325.1	127.6	121.4	153.8	209.1	152.5	136.9	186.1	301.0
1614–90	178.9	179.1	212.7	291.4	144.7	188.4	299.7	294.8	166.5	166.0	192.3	271.9	134.3	176.8	270.8	272.5
1633–0	254.6	286.3	290.1	275.2	374.9	431.6	436.0	464.8	237.6	267.4	264.7	255.0	334.6	400.0	391.1	422.8
1633–90	183.1	205.4	218.2	256.5	147.8	192.5	343.4	275.9	170.5	193.2	194.8	240.0	132.1	171.0	311.0	251.4
3750–0	221.0	221.5	263.3	325.1	211.5	237.3	282.4	287.4	207.0	208.6	242.2	305.2	197.0	224.4	257.6	269.3
3750–90	358.5	406.3	436.5	479.4	376.0	432.5	446.7	500.5	335.1	382.1	400.0	450.0	335.2	400.0	400.0	450.0
3759–0	128.6	111.5	175.9	251.9	131.9	218.9	286.2	291.4	119.6	102.6	157.1	232.8	124.7	205.9	261.2	272.7
3759–90	78.4	106.0	95.8	76.2	145.5	183.9	129.9	220.9	72.7	98.2	86.3	68.6	136.4	173.2	120.5	208.7
5815–0	319.3	398.0	317.2	275.6	400.7	438.0	412.0	326.6	298.4	374.6	285.8	254.2	335.4	400.0	370.3	290.4
5815–90	275.7	315.1	324.1	318.4	363.7	431.3	445.5	482.1	257.8	295.3	297.5	297.5	337.6	400.0	400.0	441.0
6915–0	99.8	111.3	129.2	164.5	115.7	177.9	217.8	207.7	92.6	103.7	115.3	151.8	108.9	167.6	200.9	186.0
6915–90	205.5	249.5	269.9	269.4	166.0	240.3	336.5	290.3	191.5	233.7	246.5	249.8	155.4	224.7	308.2	264.4
Average	169.7	194.0	201.8	214.1	201.8	248.5	273.0	291.1	158.1	180.8	182.2	198.0	185.3	231.0	248.1	267.9

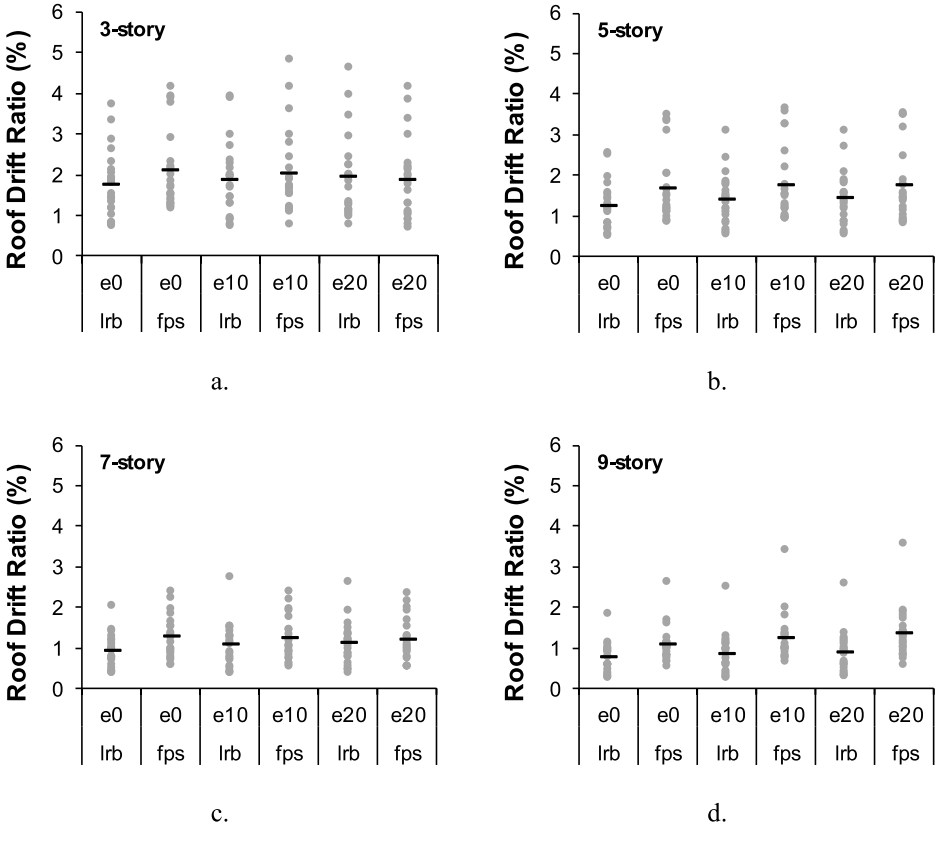

Fig. 12. Roof drift ratios of base isolated building models subjected to the scaled ground motion set.

u_{e0} corresponds to the displacement value of the e0 models in the figure. It is observed that LRB type isolators are more sensitive to torsional effects. The average displacement values of 10% and 20% eccentricity LRB type isolator models are 11% and 14% higher than the average values observed in models without eccentricity. This difference is less than 5% for FPS type isolators. It should be noted that the obtained displacement values were obtained from total displacement of building and isolators with respect to ground. Therefore, it does not reflect the superstructure displacement values.

The obtained results indicate that significant scatter exists in

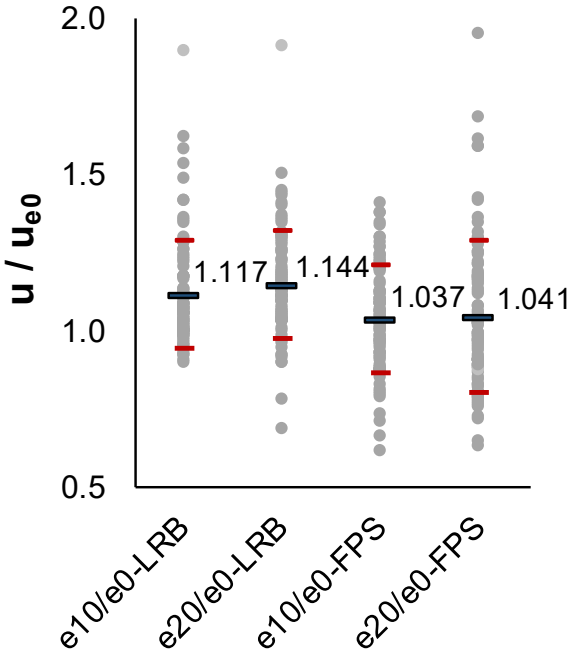

Fig. 13. The ratio of average roof displacement of models with eccentricity to the average roof displacement of models without eccentricity systems for all buildings.

displacement values of individual ground motion records for all models. The effect of eccentricity in terms of mean values is limited. Similar to the previous studies, it is observed that frequency content of several ground motion records affects the dynamic response of the base isolated system [36,56,57]. The scatter observed in Fig. 13 illustrates that the frequency content of ground motion records is effective on seismic demands especially for FPS type isolators.

The ratio of the maximum displacement of the isolator to the total displacement of the building is given in Fig. 14. Since the ratios showed a similar trend for all models, 3, 5, 7 and 9-story models were evaluated together. More than 90% of displacement values were experienced by the isolator system regardless of the eccentricity ratio and isolator type. The eccentricity due to the distribution of isolator stiffness values have very limited effect on the isolator displacement values. The displacement values of superstructure are significantly small. Therefore, the torsional effects on seismic behavior of structure are negligible. Since the eccentricity in the isolator members is much more critical, it can be predicted that the torsional irregularity on building plan will have a very limited effect. Besides, it is apparent that the base isolation system considerably decreases the superstructure displacement values as expected.

The average utilization rate of the isolator displacement capacity is given in Fig. 15. The used isolator capacities are calculated as 43.1%, 49.4% and 49.5% for e0, e10 and e20 eccentricity of LRB type isolators while these values are 63.5%, 66.3% and 66.5% for FPS type isolators. The outcomes obviously show that the capacity utilization rate of FPS type isolators modeled according to the same design displacement value is significantly higher than the LRB type isolators. When the results are analyzed separately, it is seen that the capacity utilization rate for some ground motion records were approached to 100% for FPS type isolators. Therefore, the evaluation based on average values may be misleading. Moreover, the difference between minimum and maximum capacity utilization is more striking between e0 and e10 models compared to e10 and e20 models.

4.2.1.1. Evaluation of IDR values. Interstory drift is recognized as an important damage indicator. Roof drift given in the previous section includes the displacement value of base isolator. Therefore, the evaluation of interstory drift ratio (IDR) values is important parameter to determine the superstructure displacement value. Fig. 16 compares maximum IDR values of all models. Damage limit levels defined in TBEC-2018 [41] is also illustrated on the figure as “UU” and “LD” abbreviations corresponding to uninterrupted use and limited damage limits, respectively. The controlled damage level is not shown on the figure because none of model has reached to this damage level.

When the IDR values are examined, they have similar trend with roof displacement ratios. The maximum IDR values are calculated for FPS type isolators. While none of LRB type isolator models exceeded to limited damage state, six cases of FPS type isolators are at the LD state for 3-story and 5-story models with eccentricity.

In previous studies related with base isolated systems, it is concluded that torsional irregularity may have significant effects on seismic response. However, in these studies limited number of ground motion records were considered [35,40,58]. By the nature of dynamic analysis, significant scatter in seismic demands is also observed in the scope of this study. In Fig. 17, the IDR profiles of 7-story model is given for RSN-5815 record as an example. While the differences in average results are negligible for e0 and e10 eccentricity of LRB type isolators, e10 eccentricity model estimated almost 100% higher IDR value compared to e0 eccentricity model for RSN-5815 record. A similar trend is seen for the FPS type isolator with e20 eccentricity for the same ground motion record. Since the displacement values highly depend on the nature of ground motion records, the use of several records can result in remarkably different values compared to the values of 11 pairs of ground motion records. The evaluation based on the average displacement values using 11 pairs of ground motion records indicate that effect of eccentricity is limited on the base isolated systems. Therefore, the outcomes of this study underline the careful selection of number of ground motion records in dynamic analysis as mentioned in the previous study

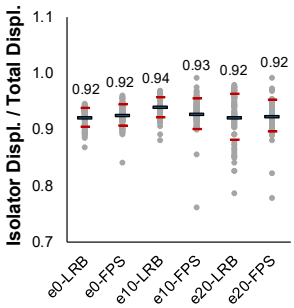

Fig. 14. Isolator displacement relative to total displacement.

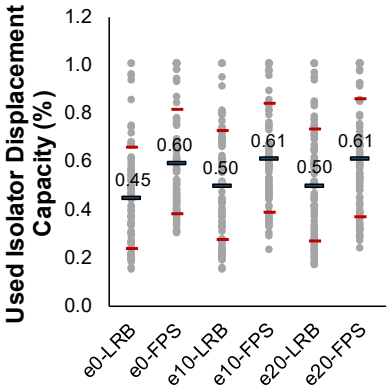

Fig. 15. The average values of the isolator displacement capacity utilization.

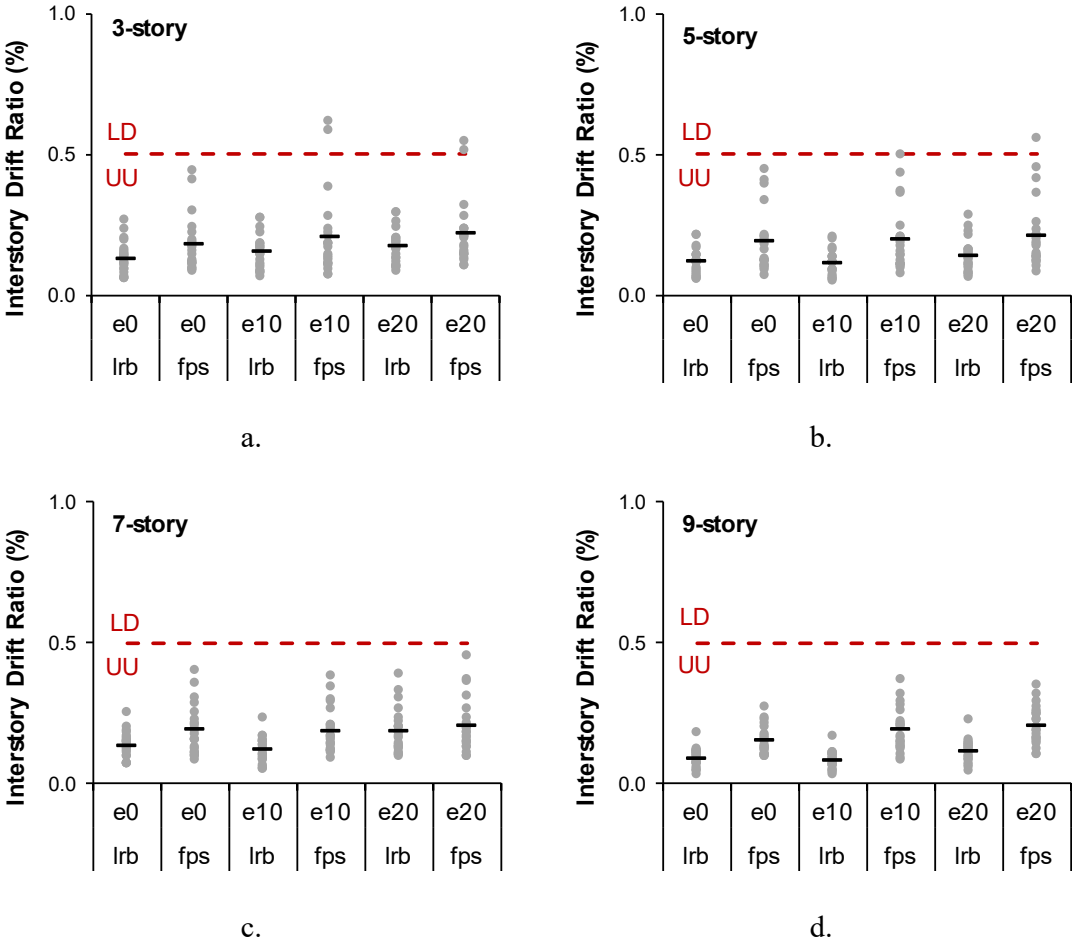

Fig. 16. Maximum interstory drift ratios for the building models.

[59].

The average IDR values of all building models are compared for models with (e10 and e20) and without (e0) eccentricity. in Fig. 18. When all models regardless of story number are evaluated together, the IDR values of the base isolated e20 models are 20% higher than that of e0 models. Although there may be cases with significant differences due to eccentricity, almost all IDR values (except few cases) are within UU damage level. Therefore, all models considered in this study may be assumed at an acceptable level considering the average IDR values.

4.2.1.2. Torsional coefficient values. Torsional coefficients defined in TBEC-2018 [41] were calculated at the time of maximum IDR and plotted in Fig. 19. The torsional irregularity coefficient limit of 1.2 is also indicated on the figure. All coefficient values are smaller than the torsional irregularity limit for models without eccentricity. As expected, the torsional irregularity coefficient values increase as the eccentricity ratio increases. Although the average coefficient values of the models with 10% eccentricity is around the limit value, there are considerable number of cases that exceed the limit coefficient value. Moreover, the average coefficient values of the models with 20% eccentricity are

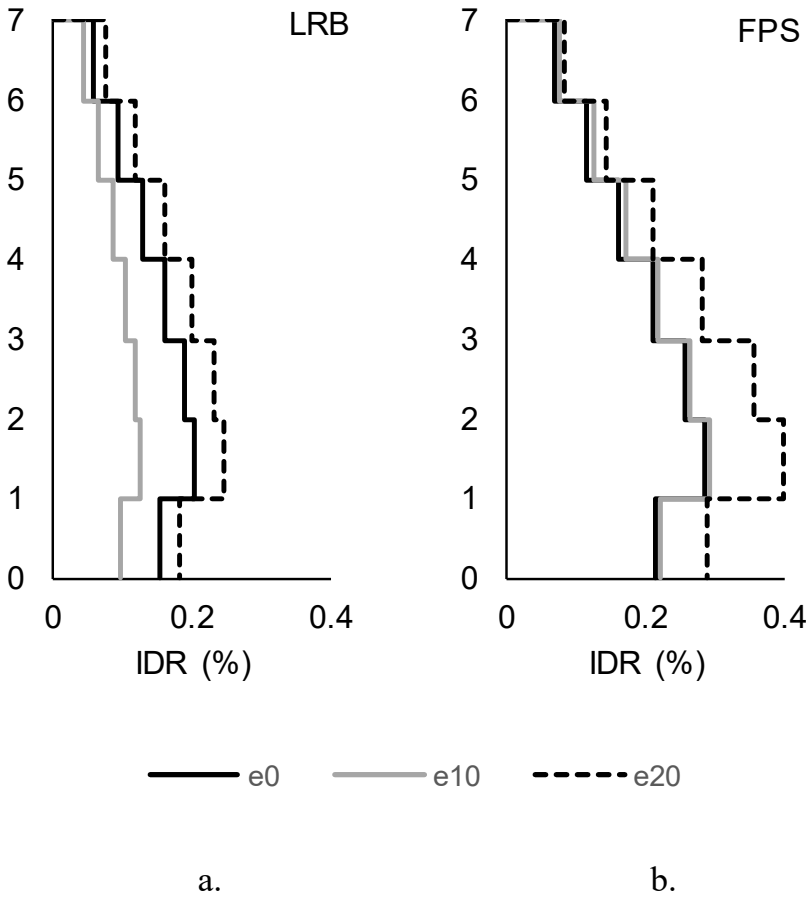

Fig. 17. IDR profiles of 7-Story model for RSN-5815 record.

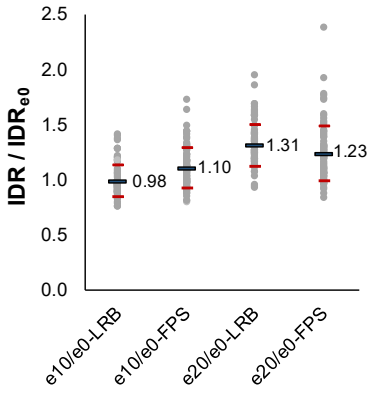

Fig. 18. IDR ratios of models with and without eccentricity.

higher than the limit value except the 3-story models. The outcomes clearly indicate that the eccentricity at the isolator triggers torsional irregularity at the superstructure. Besides, the LRB type isolators are more vulnerable to torsional irregularity compared to the FPS type isolators.

The ratio of the average coefficient values of the models with eccentricity to the models without eccentricity is given in Fig. 20. Both scatter and the average values of torsional irregularity coefficient are quite high for the LRB type isolator models. Torsional irregularity coefficient values of LRB models with 20% eccentricity are 47% higher than that of the models without eccentricity in terms of averages. The FPS type isolator models are less affected from the eccentricity.

Since significant part of the values is absorbed by the isolator system, the remaining seismic demand for the superstructure is relatively low. The variation of the torsional irregularity coefficient for RDR and IDR history is given as an example for RSN-1633 record in Fig. 21 to better understand the effects of torsional irregularity on the superstructure behavior. Since similar trends were observed in all ground motion

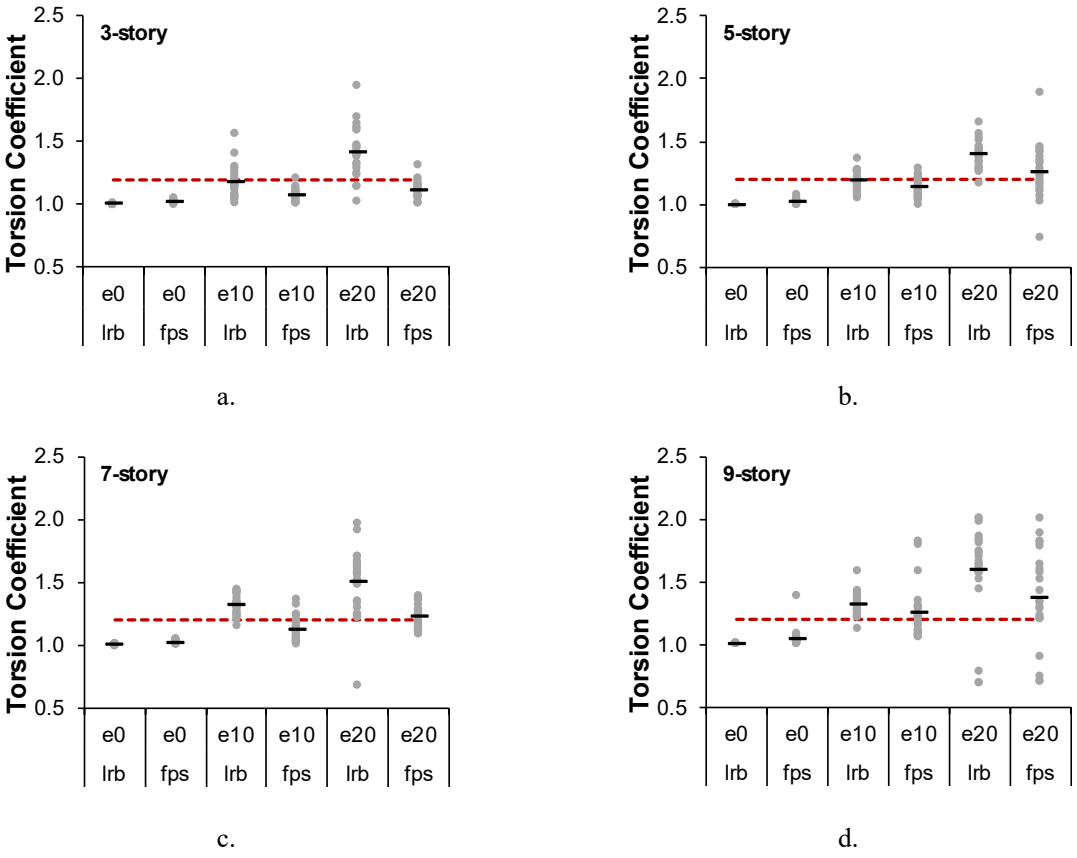

Fig 19. Torsion coefficient (η_b) for models.

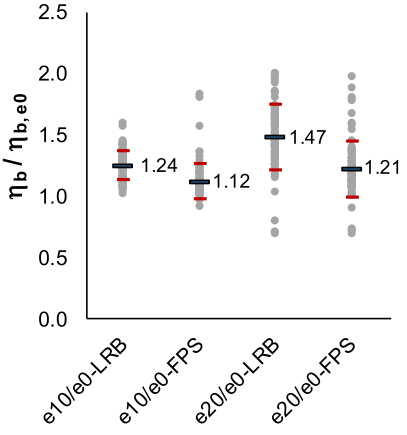

Fig. 20. Torsion coefficient (η_b) for models.

records, these graphs were not given separately for all sets. The figure illustrates the time dependent variation of the scattering of the torsional irregularity factor for the RDR and IDR values. As the eccentricity increases in base-isolation models, the frequency of torsional coefficients approaching maximum values increases significantly. Although the structural behavior is distorted by the torsional irregularity, its effect is limited due to significant damping of displacement values by the base isolator system. For this reason, it is more important to investigate the effects of torsional behavior on isolator behavior rather than superstructure behavior.

5. Conclusion

This study investigates the seismic behavior of LRB and FPS type base isolated models considering torsional irregularity for typical RC frame buildings with no shear walls. Torsional irregularity is reflected with static eccentricities due to distance between stiffness center of isolators and mass center of superstructure. For this purpose, total of 1408 different nonlinear time history analyses were performed considering 11 spectrum compatible ground motion record pairs The remarkable outcomes are summarized below:

- The highest torsional irregularity coefficients were calculated when mass center of superstructure and rigidity center of base isolator system was not coincided. Especially, placement of base isolator system directly changes the torsional behavior of superstructure.
- The eccentricities up to %20 due to the superstructure are less effective in torsional behavior.
- LRB type isolators are more sensitive to torsional effects compared to FPS type isolators. The average displacement values of LRB type isolator models with 10% and 20% eccentricities are 11% and 14% higher than the average displacement values of models without eccentricity. For FPS type isolators this difference is less than 5%. The effect of eccentricities in rubber isolated structures is dependent on the torsional frequency of the isolation system. In sliding isolation systems, when mass is offset, the center of rigidity is also offset, resulting in zero eccentricity. For these reasons it is expected that LRB type isolators are more sensitive to torsional effects compared to FPS type isolators.
- Torsional irregularity coefficient values of LRB models with 20% eccentricity are 47% higher than models without eccentricity in terms of averages. The FPS type isolator models are less affected from the eccentricity.

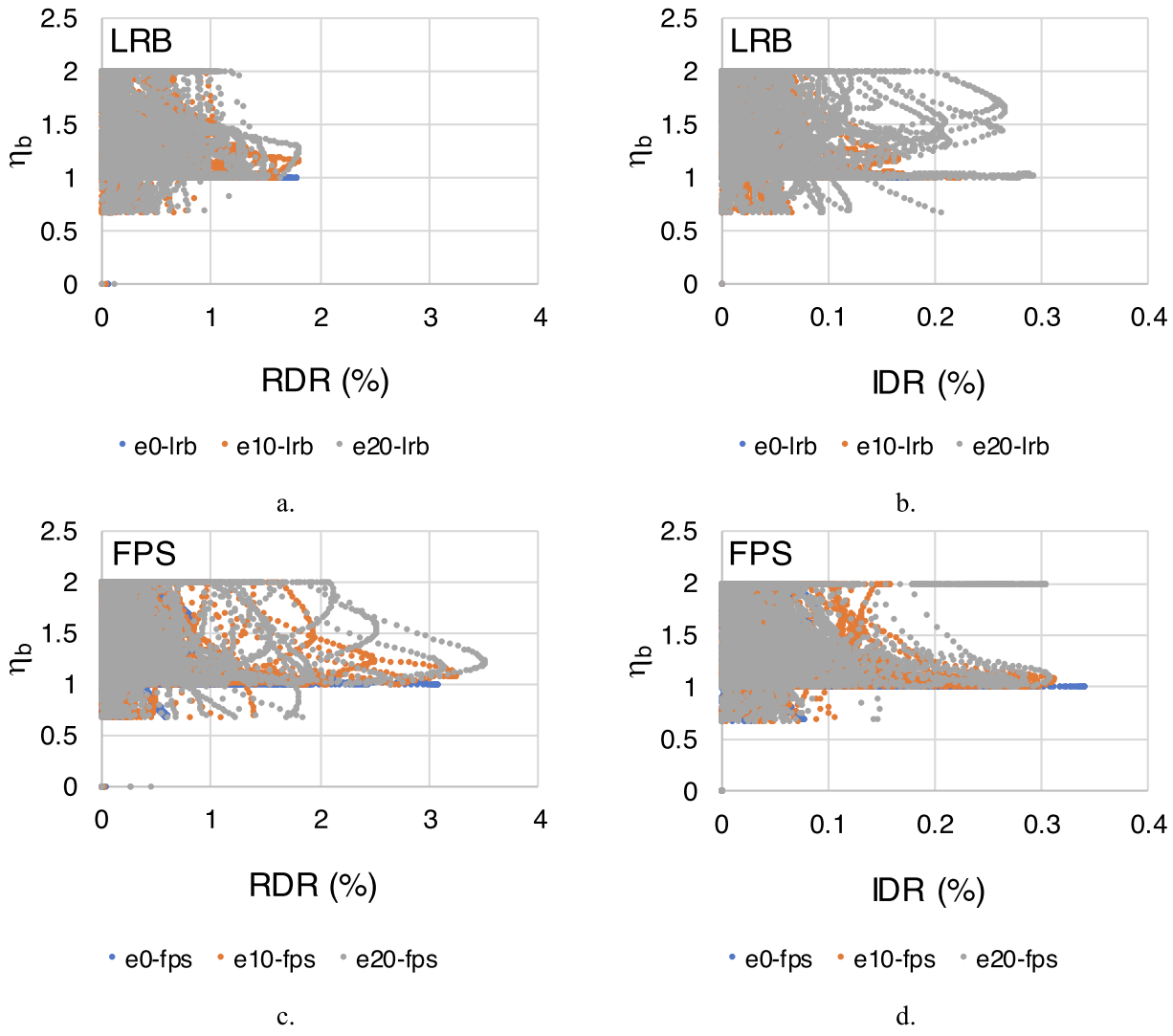

Fig. 21. Torsion coefficient (η_b) scatter for RSN-1633.

- The obtained results indicate that significant scatter exists in displacement values of individual ground motion records for all models. Using limited number of ground motion records may lead to inaccurate predictions of seismic demands.
- Since significant part of the seismic demands is absorbed by the isolator system for all models, the remaining seismic demand for the superstructure is relatively low. Therefore, the presence of irregularity in the superstructure may not affect the superstructure behavior.
- As mentioned in previous studies, it is more important to investigate the effects of torsional behavior on isolator behavior rather than superstructure behavior, especially for LRB type isolators.

Funding

No funding was received for conducting this study.

7. Availability of data and material

Not applicable.

8. Code availability (software application or custom code)

Not applicable.

9. Authors' contributions

Authors' contribution is equal.

10. Ethics approval

There is no conflict in this study.

11. Consent to participate

Not applicable.

12. Consent for publication

Not applicable.

Declaration of Competing Interest

The authors declare that they have no known competing financial interests or personal relationships that could have appeared to influence the work reported in this paper.

Acknowledgments

Not applicable.

References

[1] Ceccoli C, Mazzotti C, Savoia M. Non-linear seismic analysis of base-isolated RC frame structures. Earthq Eng Struct Dyn. 1999;28(6):633–53. https://doi.org/10.1002/(SICI)1096-9845(199906)28:6<633::AID-EQE832>3.0.CO;2-3.
[2] Erduran E, Dao ND, Ryan KL. Comparative response assessment of minimally compliant low-rise conventional and base-isolated steel frames. Earthq Eng Struct Dyn. 2011;40(10):1123–41. https://doi.org/10.1002/eqe.1078.
[3] Şengel HS, Erol H, Yavuz E. Sismik İzolasyon Tekniği ve Kullanılışına İlişkin Örnek Uygulama. J Eng Archit Fac Eskişehir Osmangazi Univ 2009;XXII:165–77.
[4] American Society of Civil Engineers (ASCE) FEMA-P-751. 2009 NEHRP Recommended Seismic Provisions: Design Examples In, Washington DC, USA, 2012.
[5] American Society of Civil Engineers (ASCE) FEMA-P-1051. 2015 NEHRP Recommended Seismic Provisions:Design Examples. In, Washington DC, USA, 2016.
[6] McVitty WJ, Constantinou MC. Property modification factors for seismic isolators: Design guidance for buildings. MCEER Rep 2015:15–0005.
[7] Heaton TH, Hall JF, Wald DJ, Halling MW. Response of high-rise and base-isolated buildings to a hypothetical Mw 7.0 blind thrust earthquake. Science 1995;267 (5195):206–11. https://doi.org/10.1126/science.267.5195.206.
[8] Clemente P. Seismic isolation: past, present and the importance of SHM for the future. J Civ Struct Heal Monit 2017;7(2):217–31. https://doi.org/10.1007/s13349-017-0219-6.
[9] Ryan KL, Kelly JM, Chopra AK. Nonlinear model for lead-rubber bearings including axial-load effects. J Eng Mech 2005;131(12):1270–8.
[10] New Zealand Society for Earthquake Enginnering(NZSEE). Guideline for the Design of Seismic Isolation Systems for Buildings. 2019. www.nzsee.org.nz/publications/design-of-seismic-isolation-systems-for-buildings.
[11] Gandelli E, Penati M, Quaglini V, Lomiento G, Miglio E, Benzoni GM. A novel OpenSees element for single curved surface sliding isolators. Soil Dyn Earthq Eng 2019;119:433–53. https://doi.org/10.1016/j.soildyn.2018.01.044.
[12] Mazza F, Mazza M. Sensitivity to modelling and design of curved surface sliding bearings in the nonlinear seismic analysis of base-isolated r.c. framed buildings. Soil Dyn Earthq Eng 2017;100:144–58. https://doi.org/10.1016/j.soildyn.2017.05.028.
[13] De Domenico D, Ricciardi G, Infanti S, Benzoni G. Frictional heating in double curved surface sliders and its effects on the hysteretic behavior: An experimental study. Front Built Environ 2019;5:1–11. https://doi.org/10.3389/fbuil.2019.00074.
[14] Constantinou MC, Whittaker ASS, Kalpakidis Y, Fenz DM, Warn GP. Performance of seismic isolation hardware under service and seismic loading. Tech Rep No MCEER-07 2007;12:471.
[15] Lomiento G, Bonessio N, Benzoni G. Effects of loading characteristics on the performance of sliding isolation devices. Proc 15th World Conf Earthq Eng 2012.
[16] Furinghetti M, Yang T, Calvi PM, Pavese A. Experimental evaluation of extra-stroke displacement capacity for Curved Surface Slider devices. Soil Dyn Earthq Eng 2021;146:106752. https://doi.org/10.1016/j.soildyn.2021.106752.
[17] Furinghetti M, Lanese I, Pavese A. Experimental assessment of the seismic response of a base-isolated building through a hybrid simulation technique. Front Built Environ 2020;6. https://doi.org/10.3389/fbuil.2020.00033.
[18] Naeim F, Kelly JM. Design of seismic isolated structures: from theory to practice. John Wiley & Sons. 1999. https://doi.org/10.1002/9780470172742.
[19] Jangid RS, Kelly JM. Base isolation for near-fault motions. Earthq Eng Struct Dyn 2001;30(5):691–707. https://doi.org/10.1002/eqe.31.
[20] Matsagar VA, Jangid RS. Influence of isolator characteristics on the response of base-isolated structures. Eng Struct 2004;26(12):1735–49. https://doi.org/10.1016/j.engstruct.2004.06.011.
[21] Ordoñez D, Foti D, Bozzo L. Comparative study of the inelastic response of base isolated buildings. Earthq Eng Struct Dyn 2003;32(1):151–64. https://doi.org/10.1002/eqe.224.
[22] Hoseini Vaez SR, Naderpour H, Kalantari SM, Fakharian P. Proposing the optimized combination of different isolation bearings subjected to near-fault ground motions. 15th World Conf Earthq Eng 2012.
[23] Mokha A, Constantinou M, Reinhorn A, Zayas VA. Experimental study of friction-pendulum isolation system. J Struct Eng. 1991;117(4):1201–17. https://doi.org/10.1061/(ASCE)0733-9445(1991)117:4(1201).
[24] Zayas, V.A.; Mahin SA. No Title. FPS Earthq. Resist. Syst. Exp. report; Earthq. Eng. Res. Cent., 1987.
[25] Almazán JL, De la Llera JC. Analytical model of structures with frictional pendulum isolators. Earthq Eng Struct Dyn 2002;31(2):305–32. https://doi.org/10.1002/eqe.110.
[26] Kelly JM. Tension buckling in multilayer elastomeric bearings. J. Eng. Mech. 2003; 129(12):1363–8. https://doi.org/10.1061/(ASCE)0733-9399(2003)129:12(1363).
[27] Sharbatdar MK, Hoseini Vaez SR, Ghodrati Amiri G, Naderpour H. Seismic response of base-isolated structures with LRB and FPS under near fault ground motions. Procedia Eng 2011;14:3245–51. https://doi.org/10.1016/j.proeng.2011.07.410.
[28] Wu YM, Samali B. Shake table testing of a base isolated model. Eng Struct 2002;24 (9):1203–15. https://doi.org/10.1016/S0141-0296(02)00054-8.
[29] Kilar V, Koren D. Seismic behaviour of asymmetric base isolated structures with various distributions of isolators. Eng Struct 2009;31(4):910–21. https://doi.org/10.1016/j.engstruct.2008.12.006.
[30] Tena-Colunga A, Escamilla-Cruz JL. Torsional amplifications in asymmetric base-isolated structures. Eng Struct 2007;29(2):237–47. https://doi.org/10.1016/j.engstruct.2006.03.036.
[31] Becker T, Keldrauk E, Mieler M. Effect of Mass Offset on the Torsional Response in Friction Pendulum Isolated Structures. 15Wcee 2003.
[32] Almazán JL, de la Llera JC. Accidental torsion due to overturning in nominally symmetric structures isolated with the FPS. Earthq Eng Struct Dyn 2003;32(6): 919–48. https://doi.org/10.1002/eqe.255.
[33] Jangid RS, Kelly JM. Torsional displacements in base-isolated buildings. Earthq. Spectra 2000;16(2):443–54.
[34] Ismail M. Elimination of torsion and pounding of isolated asymmetric structures under near-fault ground motions. Struct. Control Health Monit. 2015;22: 1295–324. https://doi.org/10.1002/stc.1746.
[35] Nagarajaiah S, Reinhorn AM, Constantinou MC. Torsion in base-isolated structures with elastomeric isolation systems. J Struct Eng. 1993;119(10):2932–51. https://doi.org/10.1061/(ASCE)0733-9445(1993)119:10(2932).
[36] Tena-Colunga A, Zambrana-Rojas C. Dynamic torsional amplifications of base-isolated structures with an eccentric isolation system. Eng Struct 2006;28(1): 72–83. https://doi.org/10.1016/j.engstruct.2005.07.003.
[37] Jangid RS, Datta TK. Nonlinear response of torsionally coupled base isolated structure. J Struct Eng 1994;120(1):1–22.
[38] Jangid RS, Datta TK. Seismic response of torsionally coupled structure with elasto-plastic base isolation. Eng Struct 1994;16(4):256–62. https://doi.org/10.1016/0141-0296(94)90065-5.
[39] Lee DM. Base isolation for torsion reduction in asymmetric structures under earthquake loading. Earthq Eng Struct Dyn 1980;8(4):349–59. https://doi.org/10.1002/eqe.4290080405.
[40] Nagarajaiah BS, Reinhorn AM, Constantinou MC, Member A. Torsional coupling in sliding base-isolated structures. J Struct Eng. 1993;119:130–49. https://doi.org/10.1061/(ASCE)0733-9445(1993)119:1(130).
[41] Turkish Building Earthquake Code (TBEC-2018). Republic of Turkey Prime Ministry Disaster and Emergency Management Authory Presidential of Earthquake Department. Ankara, Turkey (in Turkish),2018.
[42] American Society of Civil Engineers (ASCE) FEMA-P-450 (2003). Nehrp Recommended Provisions for Seismic Regulations for New Buildings and Other Structures. In, Washington DC, USA 2003.
[43] Sap 2000 CSI. Integrated software for structural analysis and design. Berkeley USA: Computers and Structures Inc; 2020. Version 2020.
[44] Cancellara D, De Angelis F. Dynamic assessment of base isolation systems for irregular in plan structures: Response spectrum analysis vs nonlinear analysis. Compos Struct 2019;215:98–115. https://doi.org/10.1016/j.compstruct.2019.02.013.
[45] Mazza F, Mazza M, Vulcano A. Base-isolation systems for the seismic retrofitting of r.c. framed buildings with soft-storey subjected to near-fault earthquakes. Soil Dyn Earthq Eng 2018;109:209–21. https://doi.org/10.1016/j.soildyn.2018.02.025.
[46] Inel M, Ozmen HB. Effects of plastic hinge properties in nonlinear analysis of reinforced concrete buildings. Eng Struct 2006;28(11):1494–502. https://doi.org/10.1016/j.engstruct.2006.01.017.
[47] SEMAp (2008) Sargı Etkisi Modelleme Analiz Programı Tubitak Proje No: 105M024 Ankara, Turkey (in Turkish).
[48] ATC-40 (Applied Technology Council). Seismic Evaluation and Retrofit of Concrete Buildings. Applied Technology Council California. 1996; Vol 1 and Vol 2.
[49] American Society of Civil Engineers (ASCE) FEMA-356 (2000) Prestandard and Commentary for the Seismic Rehabilitation of Building Rehabilitation.
[50] Pacific Earthquake Engineering Research Center (PEER) Ground Motion Database. Available at: http://ngawest2.berkeley.edu/. 2019);Accessed 19.05.2019.
[51] Haydar Kayhan A, Armagan Korkmaz K, Irfanoglu A. Selecting and scaling real ground motion records using harmony search algorithm. Soil Dyn Earthq Eng 2011;31(7):941–53. https://doi.org/10.1016/j.soildyn.2011.02.009.
[52] Karakütük Ö (2015) Effect of ground motion selection on seismic response of buildings. Master's thesis, METU, Ankara, Turkey (in Turkish).
[53] NEHRP Consultants Joint Venture. Selecting and scaling earthquake ground motions for performing response-history analyses, NIST GCR 11-917-15. In, Maryland, USA, 2011.
[54] EN 1998-2. Eurocode 8: design of structures for earthquake resistance – Part 2: bridges. Brussels: European Committee for Standardization, 2005.
[55] Seguín CE, de la Llera JC, Almazán JL. Base-structure interaction of linearly isolated structures with lateral-torsional coupling. Eng Struct 2008;30(1):110–25. https://doi.org/10.1016/j.engstruct.2007.02.019.
[56] Güner G. Bir Hastane Yapısının Klasik Yöntemle Ve Sismik İzolatör Kullanılarak Tasarımının Dinamik Yönden Karşılaştırılmasının Yapılması. PhD Thesis. Institute of Science. İTU İstanbul Turkey (in Turkish), 2012.
[57] Matsagar VA, Jangid RS. Impact response of torsionally coupled base-isolated structures. JVC/J Vib Control 2010;16(11):1623–49. https://doi.org/10.1177/1077546309103271.
[58] Tena-Colunga A, Gómez-Soberón C, Mun~oz-Loustaunau A. Seismic isolation of buildings subjected to typical subduction earthquake motions for the Mexican Pacific Coast. Earthq Spectra 1997;13(3):505–32. https://doi.org/10.1193/1.1585960.
[59] Huang Y-N, Whittaker AS. Vulnerability assessment of conventional and base-isolated nuclear power plants to blast loadings. Int J Prot Struct 2013;4(4):545–63. https://doi.org/10.1260/2041-4196.4.4.545.